Peptide Adsorption on Silica Nanoparticles: Evidence of Hydrophobic Interactions

Valeria Puddu and Carole C. Perry*

Interdisciplinary Biomedical Research Centre, School of Science and Technology, Nottingham Trent University, Clifton Lane, Nottingham NG11 8NS, U.K.

ABSTRACT Molecular recognition and interactions at the interface between biomolecules and inorganic materials determine important phenomena such as protein adsorption, cell adhesion to biomaterials, or the selective response of biosensors. Events occurring at the biomolecule–inorganic interface, despite their importance, are still poorly understood, thus limiting control of interfacial properties and response. In this contribution, using well-characterized silica nanoparticles and a series of peptides having heterogeneous physicochemical properties (S1: KLPGWSG, S2: AFILPTG, and S3: LDHSLHS) identified from biopanning against the same particles, we identify the driving forces that govern peptide–silica binding. Binding isotherms obtained by fluorimetric assay under different pH conditions allowed us to demonstrate the impact of binding environment (pH) on adsorption behavior of a given peptide–surface silica nanoparticle. Our experimental data suggest a multistep adsorption mechanism leading to the formation of multilayers on silica, in which the prevailing interactions (*i.e.*, electrostatic or hydrophobic/hydrogen bonding) and their relative contribution to the binding event are governed by the identity of the peptide itself, the substrate's surface functionality (hydrophilic or hydrophobic), and the peptide bulk concentration and solution bulk pH. Our studies show how it is possible to modulate peptide uptake on silica, or in fact on any particle, by changing either the surface properties or, more simply, the binding environment. In addition, the data reveal an intrinsic bias toward positively charged sequences in the elution conditions used in the biopanning protocol with much information about strong binder sequence diversity being lost during panning.

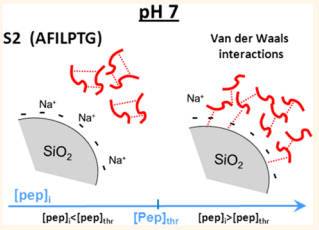

KEYWORDS: silica · peptide adsorption · hydrophobic interactions · molecular recognition · phage display

Molecular recognition and interactions at the interface between biomolecules and inorganic materials determine important phenomena such as protein adsorption, cell adhesion to biomaterials, or the selective response of biosensors. In this context, silica is a material with great commercial value and extensive technological use among both materials and biotechnology communities. Extensive experimental and computational studies performed on silica particles interacting with amino acids,[1−3] peptides,[4−6] and proteins[7,8] have identified electrostatic interactions as the principal driving force for binding. However, at the molecular level, mineral–biomolecule systems are very complex, and there are multiple parameters that might affect binding. Although considerable effort has been directed toward a general understanding of proteins binding to solids, a deep understanding of the mechanistic aspects of binding and recognition at the molecular or atomic scale is far from being achieved.[9] As a complement to information obtained from experimental studies, molecular dynamic simulations can be used to study inorganic–biomolecule interfaces with previous studies focusing on the validation and application of force fields for quartz (or other crystalline phases)–water interfaces.[10,11] Amorphous silica is, however, a very challenging material to model, due to the topographic and acidic heterogeneity of its surface.[11] The force fields available for this material are based on parameters describing bulk properties and have not been validated for biomolecule adsorption applications.[12,13]Although significant improvements have been made,[12−14] a credible force field for the amorphous silica–aqueous interface is yet to be developed and corroborated by empirical experimentally derived evidence.

Mineral-binding sequences are commonly identified using phage display libraries through an *in vivo* reiterative binding–elution process called biopanning,[15,16] originally developed for screening of biological targets. However, the complexity of the peptide–inorganic interface and the wide number of possible variables involved in the binding mechanism are reflected by the lack of convergence between binding sequences selected for materials of chemically homogeneous composition. It has recently been shown that even slight changes in the surface chemistry of a mineral can dramatically affect the peptides binding to it.[17] In the specific case of silicon

* Address correspondence to carole.perry@ntu.ac.uk.

Received for review April 27, 2012 and accepted June 24, 2012.

Published online June 24, 2012
10.1021/nn301866q

dioxide, biopanning by different authors[4−6,18] identified nonunique pools of binders whose affinity for silica was correlated with amino acid sequence and composition albeit with very limited information on the target surface structural and chemical properties being provided. As an example, Naik and colleagues[4] reported a series of 12-mer peptides rich in histidine that specifically bind "biogenic" silica (silica synthesized using the silaffin-derived peptide R5) and found that the peptides could also promote mineralization; Eteshola and co-workers[5] studied the importance of histidine at the first and sixth amino acid in peptides binding to thermally grown silicon dioxide, and Oren and colleagues used sequences isolated by biopanning against quartz powder as a starting point in a bioinformatics approach to understand sequence requirements for binding.[6] The silica substrates used in these studies (biogenic silica, thermally grown silica, and quartz), although identifiable as silicon dioxide, present different surface chemistries. Further, Patwardhan and colleagues,[18] in a recent contribution, have shown that peptides with highly dissimilar sequences bind to silica nanoparticles of apparent homogeneous synthetic origin and composition (amorphous Stöber particles) due to variations in the degree of surface ionization on particles of different size, thereby showcasing the high recognition potential of peptides for subtle differences in silica surface chemistry. Taking all of this information together, it is clear that ambiguity or limited information about the exact nature of the mineral and its surface characteristics can present a serious limitation when trying to rationalize experimental and modeling data to understand the binding mechanism at a molecular level. The poor understanding of the forces involved in binding is reflected in the difficulty to predict and control interfacial properties and response, thus limiting their technological applications.

Herein, we propose, on the basis of experimental evidence (using a well-characterized peptide−mineral model system), a binding model that rationalizes the contribution of electrostatic and nonelectrostatic forces. We demonstrate experimentally, for the first time, that once a comprehensive understanding of the possible events occurring at the interface is known, binding-dependent parameters can be intentionally manipulated to provide interfaces with a specific response or characteristics. Our approach also allowed us to highlight an intrinsic bias in the biopanning selection process toward the isolation of sequences that bind preferentially *via* electrostatic interactions, but also opens up the possibility of tuning the contribution of each distinct interaction type by choosing the environmental binding conditions to selectively favor (or avoid) specific interfacial events.

TABLE 1. Structural Properties of SiO_2 Nanoparticles

size nm	BET SA,[a] m^2/g	pore vol,[b] cm^3/g	#OH/nm^2[c]	$\xi_{pH7.4}$, mV	pzc[d]
82 ± 4	64 ± 2	0.30	4.5	−38	∼2

[a] Specific surface area determined using BET method in the range $0.05 < P/P_0 < 0.35$. [b] BJH desorption pore volume calculated between 2 and 300 nm. [c] Determined from TGA measurements. [d] Point of zero charge.

RESULTS AND DISCUSSION

In order to avoid any inconsistencies caused by changes in the material properties, a well-characterized batch of 82 ± 4 nm Stöber silica nanoparticles was used in this study (Table 1) as the target during biopanning and the subsequent adsorption assays. The nanoparticle's surface was analyzed by X-ray photoelectron spectroscopy (XPS) to rule out the presence of any contaminant that could affect the peptide adsorption. Only a low level (atomic % ≅ 1%) of contamination from hydrocarbons (C 1s binding energy: 287 eV), which may be due to prolonged exposure of the sample to the atmosphere, was detected (Figure S2 in SI).

In the biopanning experiment five rounds of selection were performed, and after the third round a progressive enrichment in clones displaying peptides S1 (KLPGWSG) and S2 (AFILPTG) was observed, S1 being the consensus sequence after five rounds (see Supporting Information Tables S1−S3). These two sequences were chosen and compared with a further peptide, S3 (LDHSLHS), which was isolated in a separate phage display experiment (Table S4) on the same silica target.[18]

The peptides selected do not display any sequence similarity and cover a range of physicochemical properties, among which is a different net charge at pH 7.4, the pH used for the panning experiments (Table 2).

In vitro silica affinity under the same conditions employed during biopanning (*i.e.*, buffered environment at pH 7.4 and the same 82 nm SiO_2 nanoparticles) was tested on the sequences prepared by solid phase synthesis (SPS). Evidence of peptide adsorption on the silica surface in the case of S3 was also given by the recorded C 1s (284.4 eV) and N 1s (399.4 eV) core level spectra at values of binding energy typical of peptides and proteins (Figure S3 and Table S5 in SI).[21] Adsorption isotherms were obtained by a fluorimetric method based on the use of fluorescamine,[18,22] which allows direct quantification of the unbound peptide and calculation of the amount of bound peptide. The adsorption experiments confirmed the affinity for silica of all three sequences isolated by phage display, Figure 1A. The measured adsorption appears to correlate inversely with the basicity of the peptide: the positively charged S1 is the "best" binder, reflecting the fact that it was isolated as the consensus sequence in the biopanning process, while neutral S2, isolated earlier

TABLE 2. Properties of Isolated Silica-Binding Peptides

peptide	sequence	pI[a]	net charge @pH 7.4	average hydrophilicity[a]	K_F	n	effect of increasing pH on binding
S1	KLPGWSG	10.1	1	−0.3	8.89	0.55	↑
S2	AFILPTG	6	0	−1	1.59	0.33	=
S3	LDHSLHS	6	−1	−0.1	0.78	0.26	↓

[a] Calculated from http://www.innovagen.se/custom-peptide-synthesis/peptide-property-calculator/peptide-property-calculator.asp.

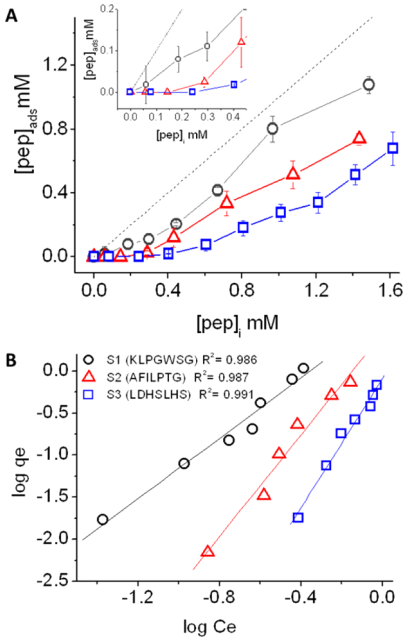

Figure 1. (A) Adsorption behavior of (○) S1 (KLPGWSG), (△) S2 (AFILPTG), and (□) S3 (LDHSLHS) on SiO_2 (82 nm). Inset: Adsorption behavior at low peptide concentration. Dotted line is theoretical 100% adsorption. (B) Freundlich fitting of isotherms for the three peptides.

in the selection process, and negatively charged S3 show lower uptake levels.

The isotherms fit the Freundlich model ($R^2 > 0.98$; Figure 1B), a commonly used empirical equation for processes of the form

$$q_e = K_F C_e^{1/n}$$

where parameter K_F is a measure of the affinity and the factor n in the exponential accounts for the intensity of the adsorption.[23] The Freundlich model is associated with multilayer adsorption,[24] with the data obtained suggesting the formation of peptide multilayers on the silica surface. This proposal was supported by calculated estimates of the peptide concentration required for monolayer coverage (based on silica particle BET surface area and the van der Waals surface of the peptides). The values required ranged from 0.05 to 0.2 μM depending on peptide orientation (flat or end on). As all adsorption experiments were carried out at concentrations that exceeded that required for monolayer coverage, strong evidence for multilayer formation on the silica surface was provided.

A different adsorption behavior at low peptide bulk concentration was found for the three peptides. S1 adsorbs on silica at concentrations as low as 0.06 mM, while S2 and S3 need to reach a threshold pep_{thr} of *ca.* 0.3 and 0.4 mM, respectively, before adsorption can be observed. (Note: a concentration of bound peptide as small as 50 nM can be detected using the fluorescamine assay.) Multilayer formation and the presence of an adsorption "lag" phase have been recently reported for isotherms on similar peptide−mineral systems.[18]

In light of data obtained from previous studies, the isolation and binding behavior of peptide S1 (KLPGWSG) is not surprising: biomolecules and polymers containing positively charged residues have been found to have high affinity for silica surfaces that display a negative surface charge at neutral pH due to the presence of deprotonated hydroxyl groups on the surface.[5,7,21] Such adsorption on the surface is entropically driven due to the release of water molecules and sodium ions from the surface.[25] However, sequences S2 (AFILPTG) and S3 (LDHSLHS) show a significant binding affinity to the silica surface despite being overall neutral (S2) and negatively charged (S3) under the conditions of the assay, indicating that different mechanisms are involved in adsorption of these peptides to the silica surface. These data support the general trend previously observed on the same substrate indicating electrostatic interactions responsible for binding of cationic peptides and nonelectrostatic and hydrogen bonds for the noncationic sequences.[18]

To probe the role of Coulomb interactions for the three silica−peptide systems, adsorption isotherms were investigated in the pH range 2.0−8.5 (Figure 2). Higher pH values were not included due to the high solubility of silica at pH values greater than 9.0. By modifying the pH of the binding environment both surface charge and net peptide charge can be tuned, thus allowing us to monitor to what extent electrostatic interactions contribute to binding of cationic S1, neutral S2, and anionic S3 peptides. The silica surface charge was evaluated experimentally by means of its zeta potential (ξ) in the pH range 2.0−9.0 (Figure 2), while for the peptides the charge was evaluated by taking into account the pK_a and dissociation ratio of the carboxyl and amino termini and of the functionalized side chains, then adding the single amino acid contributions.[26,27]

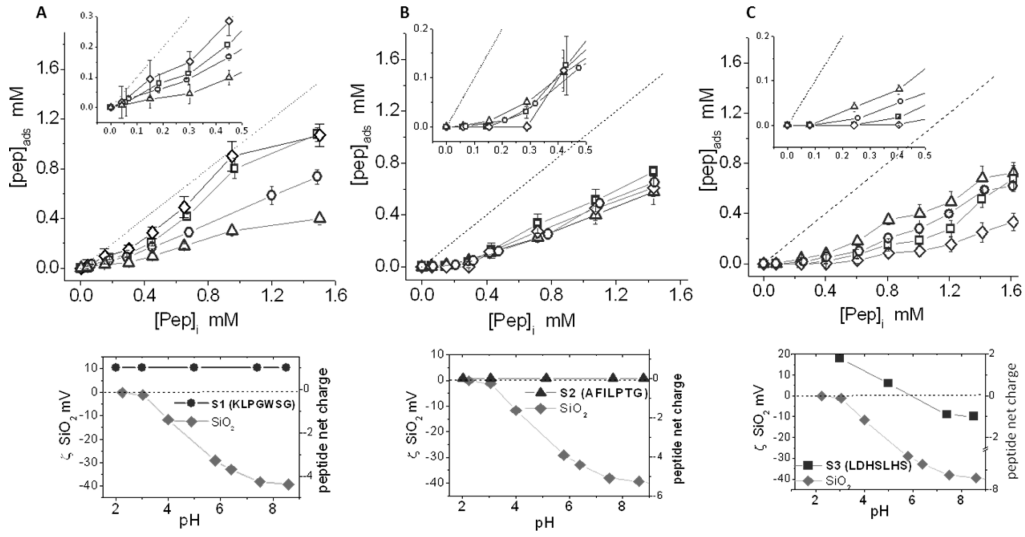

Figure 2. Adsorption isotherms at different pH values of (A) S1(KLPGWSG); (B) S2 (AFILPTG); and (C) S3 (LDHSLHS). Symbols indicate pH 3 (Δ); pH 5 (○); pH 7.4 (□); pH 8.5 (◇). The insets show the adsorption behavior at low $[pep]_i$. The charge variation as a function of pH for silica (zeta potential measurement) and the peptides (calculated values) is reported in the plots below the adsorption isotherms for each peptide.

The pH dependence of adsorption on silica was found to be sequence dependent (Figure 2) and subject to the peptide charge (Table 1). Sequence S1 (KLPGWSG) with a pI of 10.1 (mainly due to the presence of the lysine side chain containing a protonated basic amino group (pK_a = 10.4), which confers a constant +1 net charge to the peptide over the whole pH range studied) shows an adsorption increase with increasing pH, confirming the role of electrostatic forces in binding. The binding event at the molecular level most likely involves an ion-pairing mechanism[18] in which the positively charged sites on the peptide (N terminus and the lysine side chain) coordinate deprotonated silanol sites on the silica surface.

However, at conditions where Coulomb interactions are minimal, (*i.e.*, pH 3.0, where pH ≈ SiO_2 pzc) a significant uptake of S1 is observed, enabled by nonelectrostatic interactions. For binding of S1 to occur on the uncharged surface, binding forces other than electrostatic must be present. This result is important, as it shows that even the adsorption of a positively charged sequence is in fact the result of both an electrostatic and nonelectrostatic contribution, the contributions varying according to the precise experimental conditions.

Sequence S2 (AFILPTG) has a pI of 6 and is mainly constituted by nonpolar amino acids, resulting in an overall hydrophobic character. The adsorption of neutral and mainly hydrophobic S2 is essentially not pH dependent. In this case, Coulomb interactions can be excluded, and a completely nonelectrostatic mechanism between the hydrophobic domains on S2 and the silica surface (*i.e.*, siloxane bridges) is likely to occur. The dehydration of hydrophobic areas resulting from binding and the entropy gain associated with it lower the Gibbs energy of the system, driving the adsorption process.[28−30] Hydrophobic interactions are confirmed by the adsorption behavior in the low initial peptide concentration window, where a lower pep_{thr} is observed for low pH values (Figure 2B). This means that the silica−S2 interactions are favored when the silica surface is close to its pzc (*i.e.*, more hydrophobic).

Peptide S3 (LDHSLHS) has a pI very similar to that of S2, but due to the presence of the aspartic acid carboxylic acid side chain (pK_a 3.9) and two basic imidazole side chains (pK_a= 6) from histidine, the net charge of the peptide varies from +2 to −1 depending on the bulk solution pH (Figure 2C). The adsorption behavior of sequence S3 as a function of pH shows a gradual reduction of adsorption with increasing pH. The highest uptake is observed at pH ≈ SiO_2 pzc, and lower but substantial S3 binding is also observed in conditions of electrostatic repulsions (pH > 6.0). An increase in pH also results in a higher pep_{thr}. In the case of S3, at low peptide concentrations, negative electrostatic interactions prevent binding. This is supported by the increase of pep_{thr}, which is observed on increasing the pH of reaction (increasing the extent of the electrostatic repulsion in the peptide−silica system). Once pep_{thr} is reached, the main contribution to S3 peptide binding does not arise from electrostatic forces, but similarly to what was observed for S2, must arise from hydrophobic interactions and hydrogen bonding. At S3 > $S3_{thr}$ the binding observed can be attributed to a combination of nonelectrostatic events that overcome the electrostatic repulsion existing between the peptide and silica under these specific pH conditions.

In order to understand more about what is happening in solution before and during peptide binding, solutions were studied by dynamic light scattering (DLS). Measurements showed that all three peptide

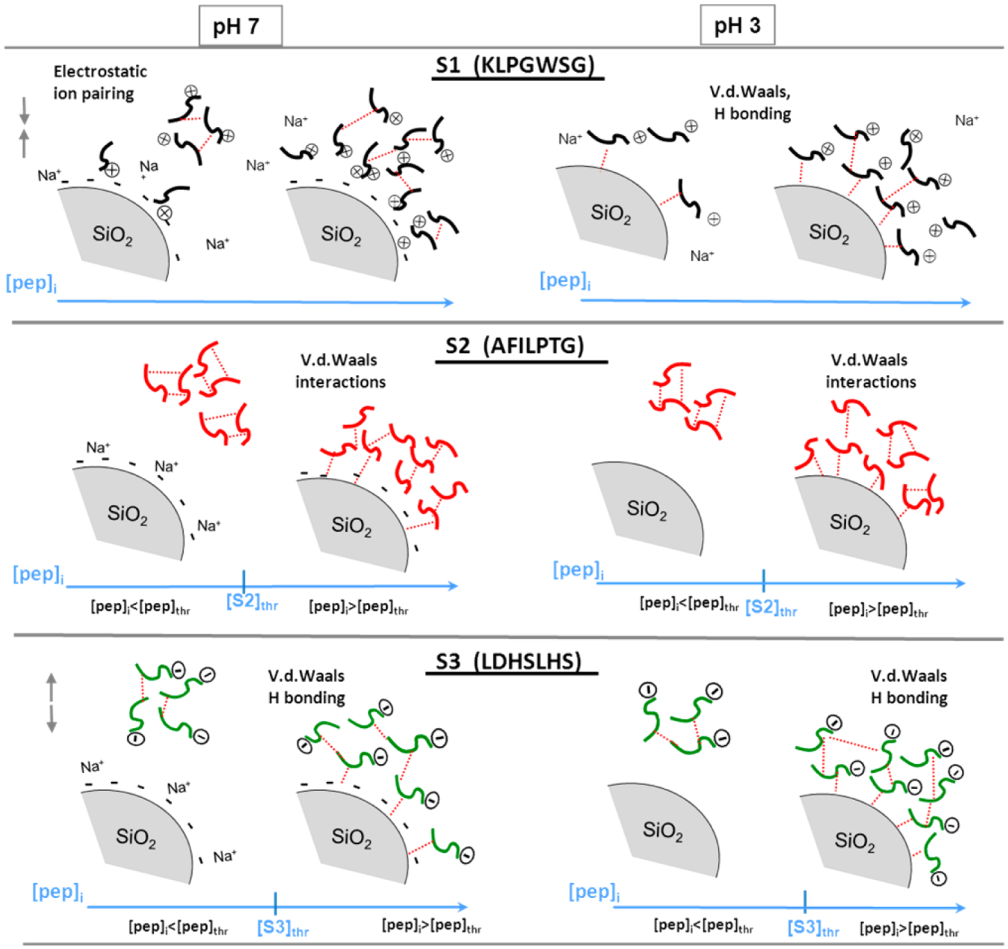

Scheme 1. Binding mechanism of a cationic S1 (KLPGWSG), neutral S2 (AFILPTG), and anionic peptide S3 (LDHSLHS) on amorphous silica nanoparticles as a function of peptide concentration and pH. Multilayers of peptides are formed in all cases due to peptide−peptide interactions.

sequences form aggregates with hydrodynamic diameters of *ca.* 250−300 nm when present in phosphate-buffered saline, independent of initial peptide concentration (Figure S1 in Supporting Information, SI). Amino acid and peptide self-association is commonly encountered in solution and is due to intermolecular H bonds, electrostatic interactions, and backbone−backbone interactions.[31,32] In the presence of silica nanoparticles, surface−peptide interactions are in competition with interactions between peptide molecules that lead to the formation of the assemblies. In a situation where the peptide surface interaction is favored, adsorption might occur through destruction of the aggregates with single peptides adsorbing on the surface or through the adsorption of the whole peptide cluster. In the case of peptides S2 and S3, the "lag" phase observed during the silica−peptide adsorption studies at low peptide concentration indicates that the aggregates stay in solution until a certain concentration is reached. In these cases, the interaction with the surface is driven by nonelectrostatic interactions and is driven largely by changes in the state of hydration of the surface and the peptides.

The above experimental results clearly reveal the contributions of hydrophobic interactions in the recognition and adsorption of differently charged peptide binders on silica at various pH conditions: for positively charged S1 when the silica surface is noncharged and for S3 in conditions of electrostatic repulsion. In particular, they are the only forces responsible for the binding of the neutral sequence S2.

The peptide silica binding event is very complex, and as emphasized in this study it depends on the many variables of the interfacial system. On the basis of our experimental results we propose a bonding model, for each sequence, shown in Scheme 1. This experimental model is strongly supported by observation from molecular dynamic simulations[18] obtained on a silica−water interface with Q^3 silica surfaces with ~4.7/nm^2 silanol and Q^3 with siloxane groups only, representing suitable models for our interfaces at pH 7.4 and 3.0, respectively. The formation of ion pairs for cationic peptides, with contribution from hydrogen bonding, polar and van der Waals interactions were identified for the simulated environment at pH 7.4, while simulations at pH 3 show only nonelectrostatic contributions to

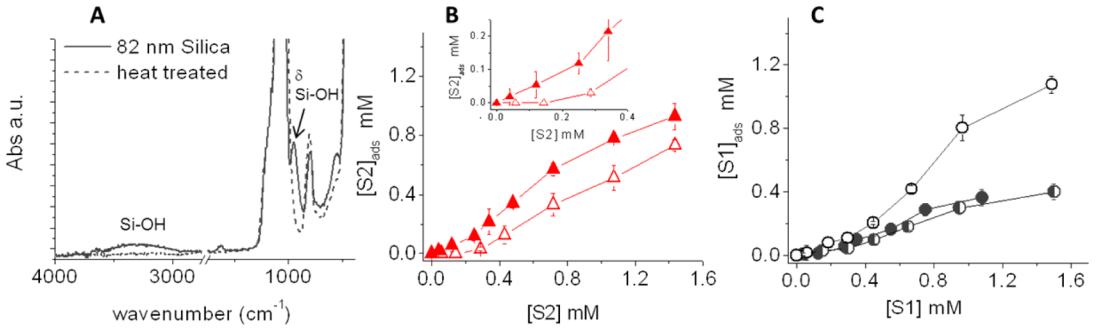

Figure 3. (A) FT-IR of 82 nm silica before (full line) and after (dotted line) heat treatment. (B) Adsorption isotherms of S2 (AFILPTG) on silica 82 nm particles before (empty symbols) and after heat treatment (filled symbols) at pH 7.4, showing a decrease of adsorption on heat-treated particles and changing of adsorption behavior at low S2 (inset). (C) Adsorption isotherms of S1 (KLPGWSG) on silica 82 nm particles before (empty symbols) and after heat treatment (filled symbols) at pH 7.4. Note that the adsorption after heat treatment is comparable with that on untreated silica particles at pH 3 (half-filled symbols).

the interactions. Our experiments clearly confirm this trend and allow us to extend this approach and predict a binding mechanism based on hydrophobic interactions for the neutral peptide S2 and anionic peptide S3.

Although van der Waals forces have been demonstrated to control the interactions between nanoparticles and nanotubes,[33] they are generally overlooked when trying to understand the behavior of biomolecule–mineral interfaces. To further validate the significance of hydrophobic interactions at the peptide silica interface, we prepared a silica surface with comparable properties but a highly hydrophobic character. Such a surface was obtained by thermal treatment of the 82 nm nanoparticles at 600 °C for 1 h, causing the loss of hydroxyl groups, as verified by FT-IR (Figure 3A), which shows the disappearance of Si–OH peaks at 950 and 3000–3500 cm^{-1}. Other properties such as surface area (BET surface area: 53 m^2/g) were comparable with those of the untreated material. We tested the adsorption behavior of both S2 and S1 on the heat-treated particles (hydrophobic surface). On the basis of the proposed mechanism, our assumption is that if a nonelectrostatic mechanism is responsible for the S2 adsorption process on the untreated particles (hydrophilic surface), peptide S2 uptake should be conserved if not improved on a comparable surface with greater hydrophobic character. As predicted, an increase in the adsorption capacity was observed, Figure 3B. Moreover, on the heat-treated particles (hydrophobic surface), S2 uptake is observed even at very low initial concentrations, while on untreated particles (hydrophilic surface) a threshold concentration had to be reached before absorption was observed to occur.

The improvement in absorption on heat-treated silica probably arises from the presence of a smaller hydration layer around the particles, thus allowing peptide molecules to more closely approach the surface and establish short-range hydrophobic interactions. Conversely, the adsorption of S1 at pH 7.4 was drastically lower on heat-treated silica, with a value

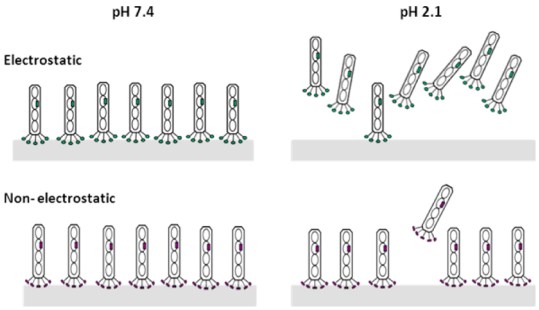

Scheme 2. Intrinsic bias of the biopanning protocol during the elution step. Silica binders interacting *via* electrostatic interactions are successfully eluted at pH 2.1, while binders interacting *via* nonelectrostatic interactions are held on the surface and resist detection.

comparable to that observed on untreated silica particles at pH 3.0 (hydrophobic surface) (Figure 3C).

The results presented above have important implications for the phage display protocol used for identification of binding sequences. In the commonly followed protocol, sequence selection is carried out at a buffered pH of 7.4, and after a series of washing cycles an elution step at pH 2.2 by Gly-HCl is performed. Under these conditions we can expect that sequences binding through electrostatic forces will efficiently be desorbed and will constitute the "tight binders" pool that will be reintroduced into the panning cycle.

We have shown that at pH 7.4 sequences bind to the silica surface by different mechanisms in a sequence- and charge-specific manner. The drop in pH used for elution disrupts the electrostatic binding interactions, allowing efficient desorption of sequences binding through electrostatic forces, but *not* those strong binders that are attached largely by means of hydrophobic or other non-Coulombic interactions (like S2). These considerations highlight an intrinsic bias toward positively charged sequences in the elution conditions used in the biopanning protocol with much information about strong binder sequence diversity being lost during panning (Scheme 2).

In light of these results, there is a necessity to develop specific elution conditions for different inorganic substrates. Further, for a given library−inorganic substrate system, the fundamental importance of the binding environment can be exploited to direct and tune specific interactions through optimization of the adsorption conditions.

CONCLUSIONS

In summary, we have shown and quantified the impact of pH on the binding behavior of differently charged peptides on amorphous silica. We have also demonstrated how the adsorption behavior of a given peptide−surface silica couple is highly sensitive to the binding environment (pH). Our experimental data suggest a multistep adsorption mechanism leading to the formation of multilayers on silica, in which the prevailing interactions (*i.e.*, electrostatic or hydrophobic/hydrogen bonding) are a function of both the binder and the substrate's surface properties as well as the peptide bulk concentration and solution bulk pH. Our studies have also shown how it is possible to modulate peptide uptake on silica, or in fact on any particle, by changing either the surface properties or, more simply, the binding environment (Figure 3C).

In this study we have studied a small number of specific sequences, and there is further work to be done exploring the role of sequence position as well as conformational effects that such changes might induce on peptide binding.[18] Such changes can be monitored by molecular simulations and together with experimental binding data will provide valuable information about the binding event(s).[18] The combined application of experimental and computational techniques will undoubtedly play a crucial role in providing a coherent picture of the effect of sequence position in these short peptides and is currently under investigation.

The outcomes of this study represent an important achievement in the establishment of general rules for binding behavior that can be extended to other systems. A further natural development of this study is the application of the same systematic approach to the study of other well-characterized interfaces.

Once a comprehensive understanding of the possible events occurring at the interface is known, binding-dependent parameters can be intentionally manipulated to provide interfaces with a specific response or characteristics.

EXPERIMENTAL SECTION

Materials and Methods. Silica nanoparticles were synthesized by a modified Stöber method.[8,19] Particle size was measured by transmission electron microscopy and averaged for 40 particles. Surface area and porosity were measured by nitrogen adsorption analysis using a Quantochrome Nova3200 on samples degassed overnight at 120 °C. Surface chemistry was analyzed by infrared spectroscopy using a Nicolet Magna IR 750 spectrometer, recording spectra at 4 cm^{-1} resolution and averaging 256 scans. ξ potential measurement were carried out on a Malvern Zetasizer Nano using a capillary cell. Thermogravimetric analysis was carried out on a Mettler Toledo TGA/SDTA851 and used to estimate the hydroxyl surface coverage of the particles on the basis of water loss at $T > 160$ °C.[20] X-ray photoelectron spectroscopy was performed on acid (HCl)-washed samples using a Surface Instruments M-probe instrument with a Al Kα source (1486.6 eV) operated at a base pressure of 3×10^{-7} Pa using step sizes of 0.01 eV (for high-resolution XPS analysis) and 1 eV (for a general XPS survey).

Biopanning. A Ph.D.-7 phage peptide display kit (New England Biolabs) was used to perform biopanning against amorphous 82 ± 4 nm SiO_2 particles following the manufacturer's instructions. Peptides identified by phage display were prepared in-house by microwave-assisted solid phase synthesis (Discover SPS microwave peptide synthesizer) as previously described elsewhere.[4]

Fluorimetric Assay. Suspensions of silica (1 mg/mL) in phosphate-buffered saline (100 mM phosphate, 150 mM NaCl) were sonicated for 1 h, suitable amounts of peptide were added in order to achieve the desired initial peptide concentration, and the mixtures were shaken vigorously. The suspension was left to equilibrate for 1 h at room temperature and then centrifuged (13 000 rpm for 5 min). The amount of peptide left in solution was quantified by fluorimetric assay. In a typical assay, 20 μL of fluorescamine (5 mg/mL in acetone) was added to a 180 μL aliquot of the supernatant in a 96-well plate, and the fluorescence intensity was measured using a Tecan Spectrafluor XFLUOR4 plate reader equipped with a 360 nm excitation filter and a 465 nm absorption filter. The concentration of each specific peptide was calculated using a peptide-specific calibration curve, and the amount of peptide adsorbed was calculated by difference from the initial peptide concentration. All assays were repeated three times in order to guarantee their repeatability.

Conflict of Interest: The authors declare no competing financial interest.

Acknowledgment. The authors thank the American AFOSR (Grant FA9550-10-1-0024) and EPSRC (EP/E048439/1) for funding this work. We are grateful to S. Jones for S3 identification and R. Naik and his research group for useful discussions and advice about phage display. J. M. Slocik (Air Force Research Laboratory, RXBN) is acknowledged for performing XPS analyses. We also thank S. Padwardhan for his contribution to assay development and initial data analysis.

Supporting Information Available: Complete list of clones identified by biopanning, DLS analysis of peptides, and XPS data. This material is available free of charge *via* the Internet at http://pubs.acs.org.

REFERENCES AND NOTES

1. Gao, Q.; Xu, W.; Xu, Y.; D., Wu; Sun, Y.; Deng, F.; Shen, W. Amino Acid Adsorption on Mesoporous Materials: Influence of Types of Amino Acids, Modification of Mesoporous Materials, and Solution Conditions. *J. Phys. Chem. B* **2008**, *112*, 2261–1167.
2. Meng, M.; Stievano, L.; Lambert, J. F. Adsorption and Thermal Condensation Mechanisms of Amino Acids on Oxide Supports. 1. Glycine on Silica. *Langmuir* **2004**, *20*, 914–923.

3. Willett, R. L.; Baldwin, K. W.; West, K. W.; Pfeiffer, L. N. Differential Adhesion of Amino Acids to Inorganic Surfaces. *Proc. Natl. Acad. Sci. U. S. A.* **2005**, *102*, 7817–7822.
4. Naik, R. R.; Brott, L. L.; Clarson, S. J.; Stone, M. O. Silica-Precipitating Peptides Isolated from a Combinatorial Phage Display Library. *J. Nanosci. Nanotechnol.* **2002**, *2*, 95–100.
5. Eteshola, E.; Brillson, L. J.; Craig Lee, S. Selection and Characteristics of Peptides that Bind Thermally Grown Silicon Dioxide Films. *Biomol. Eng.* **2005**, *22*, 201–201.
6. Oren, E. E.; Tamerler, C.; Sahin, D.; Hnilova, M.; Safar Seker, U. O.; Sarikaya, M.; Samudrala, R. A Novel Knowledge-Based Approach to Design Inorganic-Binding Peptides. *Bioinformatics* **2007**, *23*, 2816–2822.
7. Vertegel, A. A.; Siegel, R. W.; Dordick, J. S. Silica Nanoparticle Size Influences the Structure and Enzymatic Activity of Adsorbed Lysozyme. *Langmuir* **2004**, *20*, 6800–6807.
8. Roach, P.; Farrar, D.; Perry, C. C. Surface Tailoring for Controlled Protein Adsorption: Effect of Topography at the Nanometer Scale and Chemistry. *J. Am. Chem. Soc.* **2006**, *128*, 3939–3945.
9. Tamler, C.; Sarikaya, M. Genetically Designed Peptide Base Molecular Materials. *ACS Nano* **2009**, *3*, 1606–1615.
10. Lopes, P. E. M.; Murashov, V.; Tazi, M.; Demchuk, E.; Mackerell, A. D., Jr. Development of an Empirical Force Field for Silica. Application to the Quartz−Water Interface. *J. Phys. Chem. B* **2006**, *110*, 2782–2792.
11. Heinz, H.; Koerner, H.; Anderson, K. L.; Veia, R. A.; Farmer, B. L.Force Field for Mica-Type Silicates and Dynamics of Octadecylammonium Chains Grafted to Montmorillonite. *Chem. Mater.* **2005**, *17*, 5658–5669.
12. Cruz-Chu, E. R.; Aksimintiev, A.; Schulten, K. Water−Silica Force Field for Simulating Nanodevices. *J. Phys. Chem. B* **2006**, *110*, 21497–21508.
13. Van Beest, B. W. H.; Kremer, G. J. Force Fields for Silicas and Aluminophosphates Based on *ab Initio* Calculations. *Phys. Rev. Lett.* **1990**, *64*, 1955–1958.
14. Heinz, H.; Suter, U. W. Atomic Charges for Classical Simulations of Polar Systems. *J. Phys. Chem. B* **2004**, *108*, 18341–18352.
15. Dickenson, M. B.; Sandhage, K. H.; Naik, R. R. Protein- and Peptide-Directed Syntheses of Inorganic Materials. *Chem. Rev.* **2008**, *108*, 4935–4978.
16. Merzlyak, A.; Lee, S. W. Phage as Templates for Hybrid Materials and Mediators for Nanomaterials Synthesis. *Curr. Opin. Biotechnol.* **2006**, *10*, 246–252.
17. Bachmann, M.; Goede, K.; Beck-Sickinger, A. G.; Grundmann, M.; Irback, A.; Janke, W. Microscopic Mechanism of Specific Peptide Adhesion to Semiconductor Substrates. *Angew. Chem., Int. Ed.* **2010**, *49*, 9530–9533.
18. Patwardhan, S. V; Emami, F. S.; Berry, R. J.; Jones, S. E.; Naik, R. R.; Deschaume, O.; Heinz, H.; Perry, C. C. Chemistry of Aqueous Silica Nanoparticle Surfaces and the Mechanism of Selective Peptide Adsorption. *J. Am. Chem. Soc.* **2012**, *134*, 6244–6256.
19. Stober, W.; Fink, A.; Bohn, E. Controlled Growth of Monodisperse Silica Spheres in the Micron Size Range. *J. Colloid Interface Sci.* **1968**, *26*, 62–69.
20. Muller, R.; Kammler, H. K.; Wegner, K.; Pratsinis, S. E. OH Surface Density of SiO_2 and TiO_2 by Thermogravimetric Analysis. *Langmuir* **2003**, *19*, 160–165.
21. Vanea, E.; Simon, V. XPS Study of Protein Adsorption onto Nanocrystalline Aluminosilicate Microparticles. *Appl. Surf. Sci.* **2011**, *257*, 2343–2352.
22. Noble, J. E.; Knight, A. E.; Reason, A. J.; Di Matola, A.; Bailey, M. J. A. A Comparison of Protein Quantitation Assays for Biopharmaceutical Applications. *Mol. Biotechnol.* **2007**, *37*, 99–111.
23. Gregg, S. J.; Sing, K. S. W. *Adsorption, Surface Area and Porosity*; Academic Press: London, 1967.
24. Daifullah, A. A. M.; Girgis, B. S.; Gad, H. M. H. A Study of the Factors Affecting the Removal of Humic Acid by Activated Carbon Prepared from Biomass Material. *Colloids Surf., A* **2004**, *235*, 1–10.
25. Parida, S. K.; Dash, S.; Patel, S.; Mishra, B. K. Adsorption of Organic Molecules on Silica Surface. *Adv. Colloid Interface Sci.* **2006**, *121*, 77–110.
26. Moore, D. Amino Acid and Peptide Net Charges: A Simple Calculational Procedure. *Biochem. Educ.* **1985**, *13*, 10–11.
27. Nozaki, Y.; Tanford, C. Proteins as Random Coils. II. Hydrogen Ion Titration Curve of Ribonuclease in 6 M Guanidine Hydrochloride. *J. Am. Chem. Soc.* **1967**, *89*, 736–742.
28. Kotov, N. A. Layer-by-Layer Self-assembly: The Contribution of Hydrophobic Interactions. *Nanostruct. Mater.* **1999**, *12*, 789–796.
29. Ochoa, J. L. Hydrophobic (Interaction) Chromatography. *Biochimie* **1978**, *60*, 1–15.
30. Queiroz, J. A.; Tomaz, C. T.; Cabral, J. M. S. Hydrophobic Interaction Chromatography of Proteins. *J. Biotechnol.* **2001**, *87*, 143–159.
31. Harterink, J. D.; Beniash, E.; Stupp, S. I. Self-Assembly and Mineralization of Peptide-Amphiphile Nanofibers. *Science* **2001**, *294*, 1684–1688.
32. Vauthey, S.; Santoso, S.; Gang, H.; Watson, N.; Zhang, S. Molecular Self-assembly of Surfactant-like Peptides to Form Nanotubes and Nanovesicles. *Proc. Natl. Acad. Sci. U. S. A.* **2002**, *99*, 5355–5360.
33. Rance, G. A.; Marsh, D. H.; Bourne, S. J.; Reade, T. J.; Khobystov, N. N. Van der Waals Interactions between Nanotubes and Nanoparticles for Controlled Assembly of Composite Nanostructures. *ACS Nano* **2010**, *4*, 4920–4928.